

## Rectified Motion of Liquid Drops on Gradient Surfaces Induced by Vibration

Susan Daniel and Manoj K. Chaudhury\*

Department of Chemical Engineering, Lehigh University, Bethlehem, Pennsylvania 18015

Received January 3, 2002. In Final Form: March 12, 2002

When a liquid drop (1–2  $\mu\text{L}$ ) is placed on a surface possessing a continuous gradient of wettability, it moves toward the more wettable part of the gradient with typical speeds of 1–2 mm/s. This low speed arises because the driving force due to surface tension is reduced by contact angle hysteresis. The hysteresis force acting on a drop on a gradient surface is, however, spatially asymmetric—its magnitude against the gradient being larger than that along the gradient. If a periodic force is applied to a drop resting on such a gradient surface, the force against the gradient is rectified whereas it is enhanced along the gradient. This half-wave rectification of periodic force causes 1–2  $\mu\text{L}$  size drops to move with enhanced speeds of 5–10 mm/s.

It was first predicted by Greenspan,<sup>1</sup> and later by Brochard<sup>2</sup> as well as by Raphael,<sup>3</sup> that a liquid drop placed on a chemically anisotropic substrate would move toward the region of higher wettability. These predictions have subsequently been confirmed by several investigators<sup>4–10</sup> by utilizing surfaces having various types of wettability gradients. The driving force ( $F_Y$ ) for the drop movement on a heterogeneous surface comes from the gradient of the free energy of adhesion ( $\Delta G = -\pi R^2 \gamma (1 + \cos \theta)$ ) of the drop with the solid<sup>11</sup>

$$F_Y = -\frac{d\Delta G}{dx} \cong \pi R^2 \gamma \left( \frac{d \cos \theta}{dx} \right) \quad (1)$$

where  $\gamma$  is the surface tension of the liquid,  $R$  is the base radius of the drop, and  $\theta$  is the position-dependent contact angle of the liquid drop on the solid surface (as  $x$  increases,  $\theta$  decreases).

At steady state, the above force is supported by the viscous drag generated within the liquid, which, under the lubrication approximation, is<sup>2,12</sup>

$$F_V = 3\eta\pi R V \int_{x_{\min}}^{x_{\max}} \frac{dx}{\xi(x)} \quad (2)$$

where  $\eta$  is the viscosity of the liquid,  $V$  is the drop velocity,  $\xi(x)$  is the thickness of the drop, and  $x_{\min}$  and  $x_{\max}$  are two cutoff lengths, the first being of the molecular dimension and the second on the order of the drop radius. In the simplest situation, eq 2 can be integrated by assuming that the drop profile is circular.<sup>2</sup> Equating  $F_Y$  to  $F_V$  yields an expression for the steady-state velocity of the drop as

follows:

$$V \cong \frac{\gamma R \sin \theta}{3\eta \ln(x_{\max}/x_{\min})} \left( \frac{d \cos \theta}{dx} \right) \quad (3)$$

According to the Greenspan model,<sup>1</sup> which explicitly considers slippage of the liquid near the contact line,  $V$  is expressed as

$$V \cong \frac{\gamma R (d \cos \theta)}{\eta_s dx} \quad (4)$$

where  $\eta_s$  is a viscosity parameter representing the friction at the solid–liquid interface. The above treatment, however, does not take into account the effect of contact angle hysteresis. In real situations, the force originating from the free energy gradient must overcome a threshold force due to hysteresis before the drop can move.<sup>5</sup>

The effect of hysteresis on the drop motion can be estimated by calculating the force acting on a thin strip of liquid of thickness  $dy$  and integrating the force over the entire periphery of the drop, i.e.

$$F_1 = \gamma \int (\cos \theta_{aB} - \cos \theta_{rA}) dy \quad (5)$$

where  $\theta_{aB}$  and  $\theta_{rA}$  are the advancing and receding contact angles on the opposite ends of the thin strip (Figure 1).

Following Brochard,<sup>2</sup> we expand  $\cos \theta_a$  and  $\cos \theta_r$  about their values ( $\cos \theta_{a0}$  and  $\cos \theta_{r0}$ ) at the central line of the drop as follows:

$$\cos \theta_{aB} = \cos \theta_{a0} + \left( \frac{d \cos \theta_a}{dx} \right) r \quad (6)$$

$$\cos \theta_{rA} = \cos \theta_{r0} - \left( \frac{d \cos \theta_r}{dx} \right) r \quad (7)$$

Within the first-order approximation that the base of the drop is circular, eq 5, with the help of eqs 6 and 7, reduces to

$$F_1 = \pi R^2 \gamma \frac{d \cos \theta_d}{dx} - 2\gamma R (\cos \theta_{r0} - \cos \theta_{a0}) \quad (8)$$

where  $\theta_d$  is the dynamic contact angle, i.e., the macroscopically observed contact angle while the drop is in

\* To whom correspondence should be addressed.

- (1) Greenspan, H. P. *J. Fluid Mech.* **1978**, *84*, 125.
- (2) Brochard, F. *Langmuir* **1989**, *5*, 432.
- (3) Raphael, E.; *C. R. Acad. Sci. Paris, Ser. II* **1988**, *306*, 751.
- (4) Ondarucu, T.; Veyssie, M. *J. Phys. II* **1991**, *1*, 75.
- (5) Chaudhury, M. K.; Whitesides, G. M. *Science* **1992**, *256*, 1539.
- (6) Ichimura, K.; Oh, S.-K.; Nakagawa, M. *Science* **2000**, *288*, 1624.
- (7) Daniel, S.; Chaudhury, M. K.; Chen, J. C. *Science* **2001**, *291*, 633.
- (8) Bain, C. D.; Burnett-Hall, G. D.; Montgomerie, R. R. *Nature* **1994**, *372*, 414.
- (9) Domingues Dos Santos, F.; Ondarucu, T. *Phys. Rev. Lett.* **1995**, *75*, 2972.
- (10) Lee, S.-W.; Laibinis, P. E. *J. Am. Chem. Soc.* **2000**, *122*, 5395.
- (11) The change in free energy associated with the expansion of the drop is neglected in eq 3.
- (12) de Gennes, P. G. *Rev. Mod. Phys.* **1985**, *57*, 828.

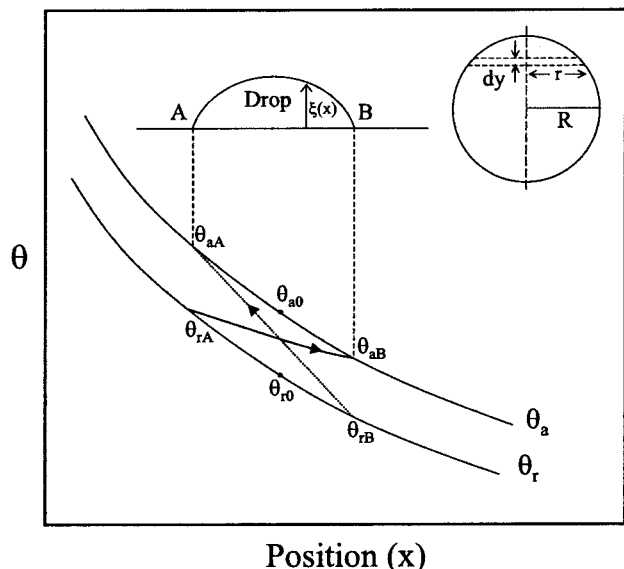


**Figure 1.** Schematics of advancing ( $\theta_a$ ) and receding ( $\theta_r$ ) contact angles of a liquid on a gradient surface. When a drop moves on this surface toward the region of higher wettability, its advancing edge experiences the angle  $\theta_{a0}$  whereas its receding edge experiences the angle  $\theta_{rA}$ . The top view of the drop, which is nearly circular on a surface of weak gradient, is shown on the right-hand corner of the figure.

motion, which is defined as follows:

$$\cos \theta_d = \frac{1}{2}(\cos \theta_a + \cos \theta_r) \quad (9)$$

Equation 8 in conjunction with eq 2 yields the velocity of drop motion on a surface in the presence of contact angle hysteresis.

The predictions of eq 3 or 4 that the velocity ( $V$ ) scales linearly with droplet radius ( $R$ ) are confirmed here by studying the movements of drops on a surface possessing a gradual variation of wettability. The gradient surface was prepared by exposing a clean glass microscope cover slip to the diffusing front of the vapor of a decyltrichlorosilane as described earlier by Daniel et al.<sup>7</sup> Once the gradient was formed, the cover slip was heated to 75 °C for 15 min to improve the bonding between the silane molecules and the substrate. The resulting surface had low wettability on its one end and high wettability on the other with a continuous variation of wettability in between (Figure 2). By carrying out several experiments, we noted that while the overall gradient property of the surface could be reproduced from one preparation to the next, it was difficult to control the hysteresis of these surfaces beyond a reproducibility of  $\pm 3^\circ$ . These small differences in hysteresis were found to have significant effects on the liquid drop velocities as discussed below.

Ethylene glycol was used as a model liquid, which provided low capillary ( $Ca < 10^{-3}$ ) and Reynolds ( $< 0.3$ ) numbers. Low capillary number ensures that the moving drop has nearly a circular profile,<sup>13</sup> whereas the low Reynolds number as well as the low aspect ratio (0.6) of the drop justifies the neglect of the momentum convection terms, which forms the basis for eq 3. Drops of ethylene glycol of various radii were deposited on the less wettable part of the gradient surface and their movements toward

(13) Within the lubrication approximation, the gradient of the curvature ( $C$ ) of the liquid surface can be represented as follows (1):  $(dC/dx) = (3Ca)/\xi^2(x)$ , where  $Ca$  is the capillary number ( $\eta U/\gamma$ ) and  $\xi(x)$  is the thickness of the liquid drop at any value of  $x$ . For low  $Ca$ , curvature is nearly constant for most parts of the drop.

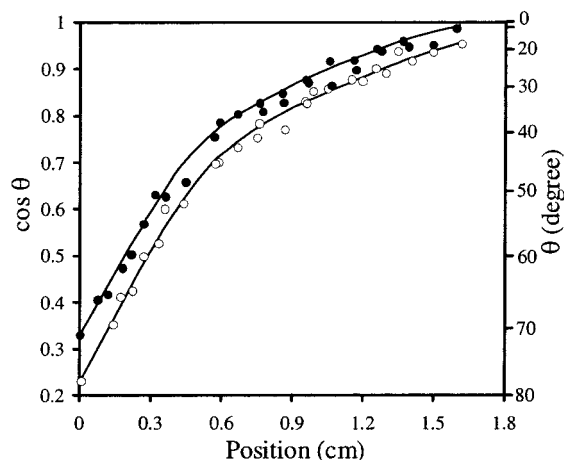


**Figure 2.** Advancing and receding contact angles of ethylene glycol on a gradient surface prepared by exposing a glass cover slip to the diffusion front of decyltrichlorosilane. (○) and (●) denote advancing and receding contact angles, respectively.

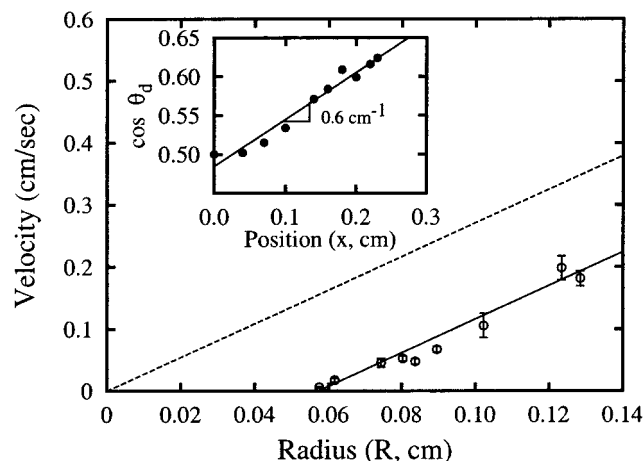


**Figure 3.** Velocities (○) of the drops of ethylene glycol on a gradient surface (Figure 2) as a function of drop radius ( $R$ ). The dashed line, which is obtained by shifting the experimental line to pass through the origin, represents the velocities to be expected in the absence of hysteresis. Variation of dynamic contact angles ( $\theta_d$ ), which were measured directly from video images of the moving drops, are shown in the inset. (Note that the  $x = 0$  position in the inset is shifted by about 0.3 mm from the zero position of Figure 2.)

the more wettable end were analyzed using a video microscopic technique. The results obtained with one of the gradient surfaces are summarized in Figure 3, which shows that the drop velocity increases linearly with the base radius as expected from eqs 3 and 4. However, below  $R = 0.055$  cm, the drops do not move, where the driving force due to free energy gradient is balanced by contact angle hysteresis. According to eq 8, this threshold point is reached when  $F_1 = 0$ , i.e.

$$\cos \theta_{r0} - \cos \theta_{a0} = \frac{\pi R}{2} \left( \frac{d \cos \theta_d}{dx} \right) \quad (10)$$

In our experiment  $(d \cos \theta_d/dx)$  is about  $0.6 \text{ cm}^{-1}$ ; using  $R = 0.055$  cm we obtain a value for the dynamic hysteresis  $(\cos \theta_{r0} - \cos \theta_{a0})$  as  $\sim 0.07$ , which is well within that measured experimentally in the quasistatic situation (Figure 2).

The above results show that hysteresis is clearly detrimental to the movements of liquid drops on a gradient surface. If it is possible to bypass the hysteresis, drops

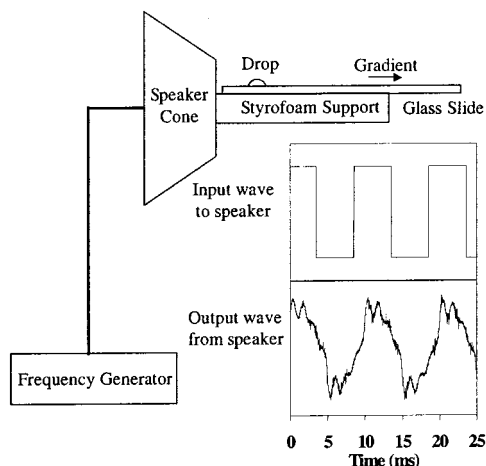


**Figure 4.** Schematics of the setup used to introduce in-plane vibration to the drop. The output wave is obtained by connecting an accelerometer to the audio speaker.

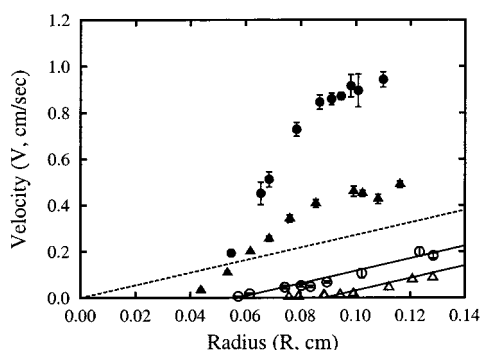


**Figure 5.** The velocities of the drops of ethylene glycol on a gradient surface are considerably enhanced in the presence of vibration. Here, the results obtained with two sets of surfaces are presented. The hysteresis of one surface (○) is 6°, while that of the other (△) is 9°. The drop velocities on these surfaces in the presence of vibration are denoted by (●) and (▲), respectively. The dashed line represents the expected velocities in the absence of hysteresis.

should move on such surfaces with speeds that are significantly higher than those reported in Figure 3. It has recently been reported that contact angle hysteresis of a liquid drop on a homogeneous surface can be mitigated by supplying additional energy to a drop by means of mechanical vibration.<sup>14–16</sup> We attempted the above approach to bypass hysteresis on a gradient surface with considerable success. In our studies, the surface was vibrated after connecting it to the transducing element of an audio speaker in such a way that an in-plane vibration could be set up on the substrate (Figure 4). The vibration was controlled by a frequency generator that produced waves of different shapes and frequency. For most parts of the current studies, square waves of 100 Hz frequency and in-plane amplitude of 40  $\mu\text{m}$  were used. The velocities of the drops during the vibration of the surface not only are an order of magnitude higher than those measured in the absence of vibration but also exceed the expected velocities when hysteresis is totally eliminated (Figure 5, dashed line).<sup>17</sup> Presumably, what we observe here is a half-wave rectification of mechanical pulses, mediated by contact angle hysteresis. The principle is illustrated with

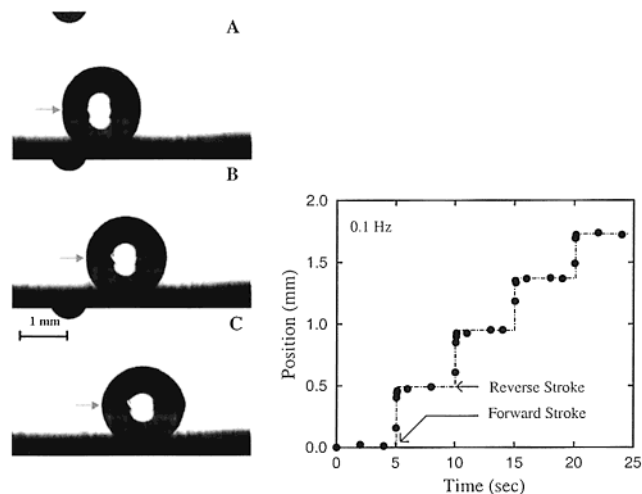


**Figure 6.** Rectified motion of a water drop is demonstrated. Here the hysteresis of contact angle is so large ( $\sim 20^\circ$ ) that the water drop of radius 1.6 mm does not move on the gradient surface. However, when the substrate is vibrated with a square wave of frequency 0.1 Hz, the drop moves in synchronization with the vibration pulse. Frame A indicates the drop at rest. Frames B and C show drop movements only toward the right during both forward and reverse strokes of the vibration. The arrow indicates the plane of reflection of the drop when it rests on the glass slide. The net movement of the drop with time has a staircase shape, as shown in the inset.

the help of Figure 1. A drop resting on a gradient surface has two ends: one coinciding with A and the other with B. Because of hysteresis, the driving force (per unit length) for the drop motion toward the more wettable part of the gradient is reduced to that given in eq 8. However, if the drop is forced to move against the gradient, a much higher force ( $F_2$ ) must be overcome

$$F_2 = \pi R^2 \gamma \frac{d \cos \theta_d}{dx} + 2\gamma R (\cos \theta_{r0} - \cos \theta_{a0}) \quad (11)$$

When the drop is vibrated mechanically, it experiences a body force during each pulse. During the acceleration phase, the body force adds to the wetting force ( $F_1$ ). However, during its deceleration, the body force is reduced by the wetting force ( $F_2$ ). No backward movement of the drop would occur if the body force during the deceleration phase is smaller than  $F_2$ . Thus, an asymmetric hysteresis on a gradient surface coupled with vibration could create a situation in which the backward movements of the drops are partially or fully rectified, whereas an attenuated bias could be set up along the wettability gradient. This situation is somewhat related to a recent phenomenon discovered by Sandre et al.,<sup>18</sup> who induced shape fluctuation to a liquid drop resting on an asymmetrically rough surface by means of an oscillatory electric field. As the equilibrium contact angle of the drop was switched between two extreme values on a sawtooth type rough surface, a rectified motion of the drop (speed  $\sim 0.15$ – $1.5$  mm/s) was observed. In our case, the asymmetry in the wetting hysteresis on the gradient surface provides the needed rectification for unidirectional drop motion. We have observed full rectified motion also with a drop of water on a gradient surface, where it initially does not move due to large wetting hysteresis ( $\sim 20^\circ$ ). However, as the surface is vibrated with a frequency of 100 Hz, the drop moves with a speed of 1 cm/s. The movement of such a drop has been closely followed by vibrating the surface at a low frequency (0.1 Hz), where no backward movement of the drop could be detected (Figure 6). We now estimate

(14) Smith, T.; Lindberg, G. *J. Colloid Interface Sci.* **1978**, *66*, 363.

(15) Andrieu, C.; Sykes, C.; Brochard, F. *Langmuir* **1994**, *10*, 2077.

(16) Decker, E. L.; Garoff, S. *Langmuir* **1996**, *12*, 2100.

(17) We note that these velocities obtained with a square wave pulse were nearly same as those obtained with a harmonic pulse.

the maximum force that acts on a drop by utilizing the simple concept of a body force in conjunction with a wetting force. Let the body force generated during each impulse be  $F$ . During the acceleration phase, the net force acting on the drop is  $F + F_1$ , whereas during deceleration, the force in the opposite direction is  $F - F_2$ . The maximum value of  $F$  that ensures no movement of the drop against the gradient is  $F = F_2$ . Thus the net force acting on the drop during the deceleration phase of the drop is zero, but is  $F_1 + F_2 = 2\pi R^2 \gamma (d \cos \theta_d / dx)$  during the acceleration phase. In the event that the wetting hysteresis is completely bypassed, the drop should not move with a speed higher than that shown by the dashed line of Figure 5. The experimental results, however, present a more complex scenario. To understand these differences, let us compare the effects of vibration on drops moving on two gradient surfaces, having slight differences ( $\sim 3^\circ$ ) in contact angle hysteresis (Figure 5). The dependence of the velocity on drop radius for the more hysteretic surface is shifted toward the right side of the radius axis as expected from eq 8. In the presence of vibration, although the drop speeds are enhanced, their magnitudes on the more hysteretic surface are nearly half of those observed with the surface

of lower hysteresis. This observation, coupled with the fact that a critical radius ( $R_c \sim 0.04\text{--}0.045$  cm) needs to be overcome for the drop to move, suggests that the effect of hysteresis is not completely eliminated by vibration. The huge enhancement of drop speed could be possible if the body force generated during vibration is itself asymmetric, i.e., when its magnitude along the gradient is significantly larger than that against the gradient. However, such a possibility could not be supported either from an examination of the waveforms or by repeating the experiment after reversing the position of the gradient surface with respect to the audio speaker. Local asymmetry may however exist in the metastable energy barriers arising due to the superposition of the wettability gradients with the corrugated energy landscapes. The complete solution of this problem however demands a stochastic description of the contact line motion requiring detailed knowledge of the surface free energy landscapes and metastable states. Further analyses along these lines are currently being attempted.

**Acknowledgment.** We thank S. Garoff for useful suggestions.

(18) Sandre, O.; Gorre-Talini, L.; Ajdari, A.; Prost, J.; Silberzan, P. *Phys. Rev. E* **1999**, *60*, 2964.

LA025505C